

## Towards a full Atmospheric Calibration system for the Cherenkov Telescope Array

M. DORO<sup>1,2,3</sup>, M. GAUG<sup>2,3</sup>, O. BLANCH<sup>4</sup>, LL. FONT<sup>2,3</sup>, D. GARRIDO<sup>2,3</sup>, A. LÓPEZ-ORAMAS<sup>4</sup>, M. MARTÍNEZ<sup>4</sup> FOR THE CTA CONSORTIUM

<sup>1</sup> *University and INFN Padova, via Marzolo 8, 35131 Padova (Italy)*

<sup>2</sup> *Física de les Radiacions, Departament de Física, Universitat Autònoma de Barcelona, 08193 Bellaterra, Spain*

<sup>3</sup> *CERES, Universitat Autònoma de Barcelona-IEEC, 08193 Bellaterra, Spain*

<sup>4</sup> *Institut de Física d'Altes Energies, 08193 Bellaterra, Spain*

*michele.doro@pd.infn.it*

**Abstract:** The current generation of Cherenkov telescopes is mainly limited in their gamma-ray energy and flux reconstruction by uncertainties in the determination of atmospheric parameters. The Cherenkov Telescope Array (CTA) aims to provide high-precision data extending the duty cycle as much as possible. To reach this goal, it is necessary to continuously and precisely monitor the atmosphere by means of remote-sensing devices, which are able to provide altitude-resolved and wavelength-dependent extinction factors, sensitive up to the tropopause and higher. Raman LIDARs are currently the best suited technology to achieve this goal with one single instrument. However, the synergy with other instruments like radiometers, solar and stellar photometers, all-sky cameras, and possibly radio-sondes is desirable in order to provide more precise and accurate results, and allows for weather forecasts and now-casts. In this contribution, we will discuss the need and features of such multifaceted atmospheric calibration systems.

**Keywords:** CTA, IACT, atmospheric calibration, remote sensing instruments

### 1 Introduction

Currently in its design stage, the Cherenkov Telescope Array (CTA) is an advanced facility for ground-based very-high-energy gamma-ray astronomy [1]. It is an international initiative to build the next-generation Cherenkov telescope array covering the energy range from a few tens of GeV to a few hundreds of TeV with an unprecedented sensitivity. The design of CTA is based on currently available technologies and builds upon the success of the present generation of ground-based Cherenkov telescope arrays (H.E.S.S., MAGIC and VERITAS<sup>1</sup>).

Nowadays, the main contribution to the systematic uncertainties of imaging Cherenkov telescopes stems from the uncertainty in the height- and wavelength-dependent atmospheric transmission for a given run of data. MAGIC cites a contribution of 10% to the uncertainty of their energy scale [2] and 12% additional uncertainty on the flux due to run-by-run variations, while H.E.S.S. retrieves 10% for the atmospheric profile, and 15% from run-by-run atmospheric variations [3]. Both estimates are based upon data recorded during clean atmospheric conditions and have to be considered lower-limits for the general case of data taken under moderately acceptable atmospheric conditions. Atmospheric quality affects the measured Cherenkov yield in several ways: The air-shower development itself, the loss of photons due to scattering and absorption of Cherenkov light out of the camera field-of-view, resulting in dimmer images and the scattering of photons into the camera, resulting in blurred images. Despite the fact that several supplementary instruments are currently used to measure the atmospheric transparency, their data are only used to retain good-quality observation time slots, and only a minor effort has been made to routinely correct data with atmospheric information [4, 5, 6].

It is envisaged that the world-wide community of scientists using CTA data will be serviced with high-level data. It is moreover foreseeable that CTA will observe many more spectral features than the current generation of Imaging Atmospheric Cherenkov Telescopes (IACTs), probably also resolving finer structures. To achieve this goal, the atmosphere must be monitored continuously and precisely such that observatory data can be corrected before dissemination. This requires the extensive use of remote-sensing instrumentation such as LIDARs, possibly complemented by additional atmospheric monitoring devices to complement the LIDAR information.

### 2 Effects of atmospheres on data reconstruction

Although IACTs are normally placed at astronomical sites, characterized by extremely good atmospheric conditions, the local atmosphere is potentially influenced by phenomena occurring at tens to thousands of kilometers far, and thus should be continuously monitored. Of the various atmospheric layers, only the troposphere (reaching up to ~15 km) and sometimes parts of the tropopause and, in the case of stratovolcanic eruptions, the lower stratosphere (15–20 km) are affected by variations of their chemical (and thus optical) properties. Air molecules can travel to the top of the troposphere (from 7 to 20 km depending on the latitude) and back down in a few days, hence this mixing makes the characteristics of the layer changing fast. While the molecular content of the atmosphere varies very slowly at a given location during the year, and slowly from place to place, aerosol concentrations can vary on time-

1. [www.mpi-hd.mpg.de/hfm/HESS/](http://www.mpi-hd.mpg.de/hfm/HESS/),  
[wwwmagic.mppmu.mpg.de](http://wwwmagic.mppmu.mpg.de),  
[veritas.sao.arizona.edu](http://veritas.sao.arizona.edu)

scales of minutes and travel large, inter-continental, distances. Most of them are concentrated within the first 3 km of the troposphere, with the free troposphere above being orders of magnitude cleaner. Aerosol sizes reach from molecular dimensions to millimeters, and the particles remain in the troposphere from 10 days to 3 weeks. The sizes are strongly dependent on relative humidity. Different types of aerosol show characteristic size distributions, and an astronomical site will always show a mixture of types, with one possibly dominant type at a given time and/or altitude. Light scattering and absorption by aerosols needs to be described by Mie theory or further developments of it, including non-sphericity of the scatterer. Aerosols use to have larger refraction indices than the one of water, and typically show also a small imaginary part. Contrary to the typical  $\lambda^{-4}$  wavelength dependency of Rayleigh-scattering molecules, aerosols show power-law indices (the so-called *Ångström* coefficients) from 0 to 1.5, i.e. a much weaker dependency on wavelength.

In order to estimate the effect of different atmospheric conditions on the image analysis of IACTs, we have simulated different molecular and aerosol profiles for the MAGIC system, consisting of two telescopes. The results are presented elsewhere in this conference [7]. Several aerosol scenarios have then been simulated: Enhancements of the ground layer from a quasi aerosol-free case up to a thick layer which reduces optical transmission by 70%, a cloud layer at the altitudes of 6 km, 10 km (cirrus) and 14 km (volcano debris) a.s.l. and a 6 km cloud layer with varying aerosol densities. We found — as expected — that the aerosol and clouds layer height, besides the density and type, affect the data differently, and that the position of this overdensity should be known precisely. In other words, the *total* extinction (or the Aerosol Optical Depth) is not a good parameter for all cases, and using only integral extinction often may lead to large systematic errors. For this reason, height-resolving instruments are required. We believe that the main findings of this study should also be valid for CTA, at least in the energy range from 50 GeV to 50 TeV, albeit efforts have started to repeat the same simulations for CTA. Previous studies have been made [8, 4, 5] for H.E.S.S. and for the MAGIC mono system, however only for an increase of low-altitude aerosol densities, and in [9] for a reference configuration of CTA, claiming a change in the spectral power-law index of gamma-ray fluxes, when atmospheric aerosol layers are present. In our work, we found that different atmospheres affect the energy threshold, the energy resolution and the energy bias, that propagate into the computation of a target flux and spectral reconstruction. See [7] for further details.

### 3 Raman LIDARs for CTA

Atmospheric properties can be derived, to a certain extent, directly from IACT data. Several studies have been made by the H.E.S.S. and MAGIC collaborations to estimate the integral atmospheric transmission, using trigger rates, muon rates, combinations of both [6], or the anode currents of the photomultipliers and/or pedestal RMS. Up to now, these parameters have been used only to discard data taken under non-optimal conditions, but work is ongoing to use this information to correct data themselves. However, as stated above, the use of integral transmission parameters is only valid in some of the possible atmospheric scenarios, namely those where the aerosol enhancement is found at the ground layer, or where clouds are low (below few k-

m a.g.l.), since the integral transmission parameters lack information about the layer height. For layers at higher altitudes, trigger rates with different cuts in image size and the stereo shower parameters themselves could eventually be used, however studies on these possibilities are not yet conclusive. For this reason, we have investigated the possibilities of using remote sensing devices such as the LIDAR [16].

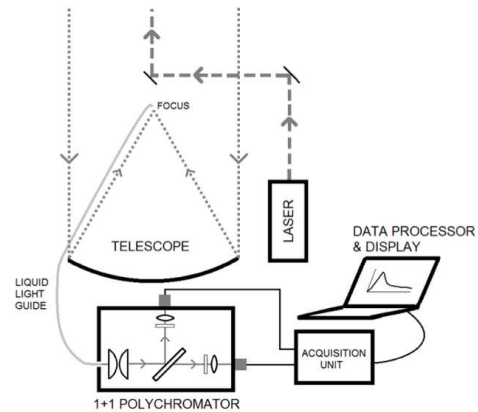


**Fig. 1:** Schematic view of a possible Raman LIDAR for the CTA. A laser is pointed towards the atmosphere, and the backscattered light collected by a telescope. At the focal plane, a light guide transports the light to a polychromator unit which is controlled and readout by an acquisition system and a data processor unit.

LIDAR is an acronym for Light Detection And Ranging. The methodology of the LIDAR technique requires the transmission of a laser-generated light-pulse into the atmosphere (see Fig. 1). The amount of laser-light backscattered into the field of view of an optical receiver on the ground, is then recorded and analyzed. LIDARs have proven to be a powerful tool for environmental studies. Successful characterization of the atmosphere has been made at night using these systems [10, 11, 12], and in other fields of astronomy, the LIDAR technique has proven to be useful for the determination of the atmospheric extinction of starlight [13]. Of the various kinds of LIDARs, the so-called elastic one make only use of the elastically backscattered light by atmospheric constituents, while the Raman LIDARs make also use of the backscattered light from roto-vibrational excitation of atmospheric molecules. Elastic LIDARs are the simplest class of LIDAR, but their backscatter power return depends on two unknown physical quantities (the total optical extinction and backscatter coefficients) which need to be inferred from a single measurement. As a result various assumptions need to be made, or boundary calibrations introduced, limiting the precision of the height-dependent atmospheric extinction to always worse than 20%. The introduction of additional elastic channels and/or Raman (inelastic-scattering) channels allows for simultaneous and independent measurement of the extinction and backscatter coefficients with no need for *a priori* assumptions [11]. Raman LIDARs yield a precision of the atmospheric extinction of better than 5%.

The LIDAR return signal can be fully described by the LIDAR equation:

$$P(R, \lambda_{rec}) = K \frac{G(R)}{R^2} \beta(R, \lambda_{em}) T^\uparrow(R, \lambda_{em}) T^\downarrow(R, \lambda_{rec}) \quad (1)$$

which contains a system factor  $K$  (emitted power, pulse duration, collection area of the telescope), a geometrical overlap factor (overlap of the telescope field-of-view with the laser light cone)  $G(R)$ , the molecular and aerosol backscatter coefficient  $\beta(R, \lambda_{em})$  and the transmission terms  $T^\uparrow(R, \lambda_{em})$  and  $T^\downarrow(R, \lambda_{rec})$ .  $R$  is the atmospheric range, i.e. the distance from the LIDAR optical receiver, and  $\lambda_{em,rec}$  are the emitted and received wavelengths.

Using the elastic and Raman-scattered profiles, the atmospheric aerosol extinction coefficients  $\alpha^{m,p}$  ( $m$  stands for molecules and  $p$  stands for particles or aerosol) can be derived using formulas such as:

$$\alpha^p(R, \lambda_0) = \frac{\frac{d}{dr} \ln \left( \frac{N_{N_2}(R)}{R^2 P(R, \lambda_{N_2})} \right) - \alpha^m(R, \lambda_0) - \alpha^m(R, \lambda_{N_2})}{1 + \left( \frac{\lambda_0}{\lambda_{N_2}} \right)^A} \quad (2)$$

where  $\lambda_0$  is the elastic wavelength (355, 532 nm in our case) and  $\lambda_{N_2}$  is the corresponding Raman-shifted  $N_2$  backscattered wavelengths (387, 607 nm).  $N_{N_2}$  is the nitrogen number density. Eq. (2) has only the Ångström index as free parameter (if only one elastic-Raman wavelength pair is used) and this leads to a good precision on  $\alpha^p$ , because over- and underestimating the Ångström index by 0.5 leads to only 5% relative error in the extinction factor. Hence, apart from statistical uncertainties (which can be minimized by averaging many LIDAR return signals), results are typically precise to about 5-10% **in each altitude bin**, and probably even better in clear free tropospheres with only one aerosol layer. The uncertainty generally grows with increasing optical depth of the layer. By adding a **second Raman line**, e.g. the  $N_2$  line at 607 nm, the last free Ångström parameter becomes fixed, and precisions of **better than 5%** can be achieved for the aerosol extinction coefficients. The molecular extinction part needs to be plugged in by hand using a convenient model. However, since the molecular densities change very little, and on large time scales, this can be achieved by standard tools. Precisions of typically better than 2% are rather easy to achieve.

The experience of MAGIC with an elastic LIDAR system (i.e. analyzing only one backscatter wavelength, and no Raman lines), has shown that simplified reconstruction algorithms can be used to achieve good precision of the aerosol extinction coefficients, at least within the range of uncertainties inherent to an elastic LIDAR [14]. An analog conclusion was achieved with the H.E.S.S. LIDAR: a stable analysis algorithm was found, limited by the 30% uncertainties of the time and range dependent LIDAR ratio.

#### 4 Raman LIDAR characterization

Several institutes in CTA are currently designing Raman LIDAR systems: the Institut de Física d'Altes Energies (IFAE) and the Universitat Autònoma de Barcelona (UAB), located in Barcelona (Spain), the LUPM (Laboratoire Univers et Particules de Montpellier) in Montpellier (France) and the CEILAP (Centro de Investigaciones Laser y sus Aplicaciones) group in Villa Martelli (Argentina) [15]. The different groups are designing independently the LIDAR systems with different mechanical, optical and steering solutions. In order to assess the performance of Raman L-

IDARs for CTA, we use the current baseline design of the Barcelona LIDAR, which is also presented elsewhere in this conference [16]. It consists of a 1.8 m diameter parabolic mirror equipped with a powerful Nd:YAG laser. The outgoing laser beam at 355 and 532 nm is directed towards the telescope pointing axis in a co-axial configuration, ensuring full near-range overlap at little more than hundred meters. In the design of the optical readout module, special care has been taken to minimize signal losses throughout the entire light collection scheme, especially for the 2 dim Raman lines at 387 and 607 nm. For the Barcelona LIDAR, a so-called *link-budget* figure-of-merit calculation has been performed showing that the dimmest Raman line will be detected from a distance of 15 km (see Fig. 2) with a signal-to-noise ratio of 10 after only one minute. This short integration time (non standard for typical LIDAR usage) is required for CTA because the LIDAR operation should not interfere with the experiment datataking. For example, it could be possible to perform LIDAR campaigns entirely during the telescope repositioning time.

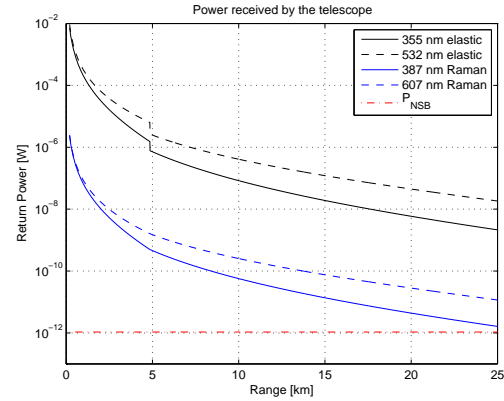


**Fig. 2:** Estimated return power from the link-budget simulation of the Barcelona Raman LIDAR. The horizontal red line is the background power calculated for a typical night-sky background at an astronomic site.

#### 5 Strategies for data reconstruction

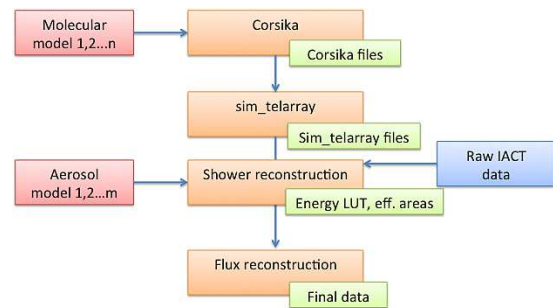


**Fig. 3:** Scheme of a possible data analysis flow in case the atmospheric model is used at the data level.

Once the atmospheric extinction profile is determined, the data taken with the CTA observatory need to be corrected accordingly. This can be achieved by re-calibrating the data themselves, either event-wise or bin-wise (Fig. 3), or

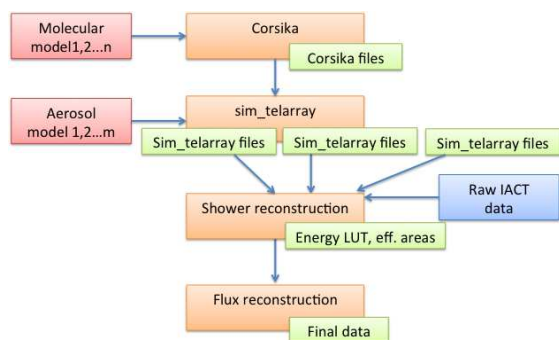


**Fig. 4:** Scheme of possible data analysis flow where the atmospheric information is introduced in the Monte Carlo simulations

by simulating adapted atmospheres (Fig. 4). We have seen from our simulations that data affected by enhancements of the ground layer can be scaled rather easily up to high levels of extinction, and probably no dedicated MC simulation is needed for each set of data. This is not the case anymore for (cirrus) clouds at altitudes from 6 to 12 km a.s.l., which create strong energy-dependent effects on the scaling factors. Moreover, the images are distorted depending on the location of the shower maximum, which varies even for showers of a same energy. Very high altitude layers, in turn, produce only effects on the very low energy gamma-ray showers. Depending on the properties of the chosen site for CTA, still to be decided, it would probably make sense to create 10 – 20 typical atmospheric simulations within these possibilities and interpolate between them.

## 6 Complementing devices

Apart from the Raman LIDAR, complementary devices for atmospheric characterization and the understanding of the site climatology can be used. A first class of devices comprises those which provide at least some profiling of the atmosphere, such as radio sondes, profiling microwave or infrared radiometers and differential optical absorption spectrometers. The operating wavelengths of these devices are very different from those of the Raman LIDAR, and precise conversion of their results to the spectral sensitivity window of the CTA is difficult. However, since aerosols are better visible at larger wavelengths, profiling devices may be used to determine cloud heights with high precision and their results may be good seeds for the Raman LIDAR data inversion algorithm. A next class of complementary devices contains those which measure integral parameters, such as Sun, Lunar and stellar photometers, UV-scopes and starguiders. Integral optical depth measurements have become world-wide standards, organized in networks ensuring proper (cross-)calibration of all devices. Spectacular resolutions of better than 1% can be obtained during the day, about 2% with moon, and 3% under dark night conditions, at wavelength ranges starting from about 400 nm. Extrapolations to the wavelength range between 300 and 400 nm worsens the resolution again. The precise results from these devices can serve as important cross-checks of the integrated differential Raman LIDAR transmission tables. Finally, all major astronomical observatories operate cloud detection devices, mainly all-sky cameras and/or take advantage from national weather radars. All-sky cameras have become standardized within the CONCAM or

the TASCA networks, however important differences in sensitivity to cirrus clouds are reported. The advantage of these devices are their big field-of-view which allows to localize clouds over the entire sky and makes possible online adapted scheduling of source observations. Relatively cheap cloud sensors based on pyrometers or thermopiles have been tested by the MAGIC collaboration and the SITE WP of CTA. The calibration of these devices is however complex and measurements are easily disturbed by surrounding installations. Recent analysis can be found in [17, 18].

## 7 Conclusions

The CTA observatory will have two arrays of telescopes, one in Southern and one in the Northern hemispheres not chosen yet. Despite the astronomical sites are expected to have extremely good atmospheric conditions for most of the year, with dry clean air, the experience with H.E.S.S., MAGIC and VERITAS has shown that non-monitored atmospheric variations introduce systematic effects on the data, which limit the energy and flux reconstruction. With the goal of producing high-quality data for CTA, currently various groups are developing instruments for atmospheric monitoring and calibration. In particular, our Monte Carlo studies have shown that integral atmospheric transmission parameters are not sufficient to fully characterize the atmosphere (related to the fact that gamma-ray showers are initiated at altitudes between the strato- and troposphere) and that range-resolved measurements are advisable. The natural solution is the use of (Raman) LIDARs, which were described in this contribution. In addition, the use of complementary instruments that measure integral or differential (in altitude) atmospheric parameters is possible and envisaged. Once retrieved the differential atmospheric transparency, different strategies are foreseen to accurately and precisely reconstruct data, ultimately reducing the reconstructed energy and flux uncertainties. In addition, it would be possible to increase the duty cycle of the telescopes by retrieving those data taken during non-optimal atmospheric conditions which are normally discarded by standard clean-atmosphere analysis, especially important during e.g. multi-wavelength campaigns or target of opportunity observations. Finally, the use of atmospheric instruments will allow for continuous weather now- and forecast.

**Acknowledgment:** We gratefully acknowledge support from the agencies and organizations listed in this page: <http://www.cta-observatory.org/?q=node/22>

## References

- [1] M. Actis et al., *Exper.Astron.* 32 (2011) 193-316.
- [2] J. Aleksić et al., *Astrop.Phys.* 35 (2012) 435-448
- [3] F. Aharonian et al., *A&A* 457 (2006) 899-915
- [4] S. J.Nolan et al., *Procs.* 30th ICRC (2007)
- [5] D. Dorner et al. *A&A* 493 (2009) 721-725
- [6] R. De Los Reyes et al, these proceedings, ID-0610
- [7] D. Garrido et al., these proceedings, ID-0465.
- [8] K. Bernlöhr, *Astrop.Phys.* 12 (2000) 255-268
- [9] S.J. Nolan et al., *Astrop.Phys.* 34 (2010) 304-313
- [10] H. Inaba, Springer-Verlag, New York (1976) 143
- [11] A. Ansmann et al., *Appl.Opt.* 31 (1992) 7113
- [12] A. Behrendt et al., *Appl.Opt.* 41 (2002) 7657
- [13] P.C. Zimmer et al., *Procs.* AAS Meeting, 42 (2010) 401
- [14] C. Fruck et al., these proceedings, ID-1054.
- [15] P. Ristori et al., these proceedings, ID-0346.
- [16] A. Lopez-Oramas et al., these proceedings, ID-0210.
- [17] M. Daniel and G. Vasileiadis, *AIP Conf. Procs.* 1505 (2012) 717-720
- [18] J. Hahn et al., *AIP Conf. Procs* 1505 (2012) 721-724